NUMERICAL SIMULATION OF STRESS BEHAVIOR DURING SHOT PEENING

K. IKUSHIMA*, Y. YAMADA*, M. SHIBAHARA*,
S. NISHIKAWA** and K. AKITA***

**Osaka Prefecture University*
***Iwate University*
****Tokyo City University*

DOI 10.3217/978-3-85125-615-4-23

ABSTRACT

Welding is widely used in the manufacture of steel structures. But welding causes residual tensile stress. Residual stresses due to welding may affect the initiation of fatigue cracks and stress corrosion cracking. These defects have significant effect on the integrity of products. In order to reduce or mitigate the tensile residual stress, surface treatment by peening has been proposed. To guarantee the safety of the products, it is important to evaluate the effect of peening on the surface stress in advance of fabrication. In this study, we proposed a method to predict the reduction of tensile residual stress due to shot peening using finite element method. The proposed method was applied to the analysis of Almen strip piece. In the analysis, the relation between the amount of shot projection and the arc height was discussed. In addition, the proposed method was also applied to the analysis of the shot-peened bead-on-plate specimen. As a result, we confirmed that the proposed method can quantitatively predict shot peening and it can analyse the effect of reduction of welding residual stress of tension by shot peening.

INTRODUCTION

Welding is widely used to join members in the manufacture of steel structures, but it is known that strong tensile residual stress can be generated on the surface by welding [1-3]. Residual stress is considered to be one of the major cause of the initiation of fatigue crack and stress corrosion cracking (SCC). Those severe defects many influence the integrity of the structure. So, it is important to reduce or mitigate the residual tensile stress in the structure due to welding.

Various peening techniques using a laser, shot, water jet have been proposed in order to modify the tensile residual stress of the surface of welding construction [4-6]. In these peening methods, an impact force is applied to the surface of the target, and this generates an elongating plastic strain in the in-plane direction by a strong compressive force in the normal direction due to the impact. A compressive stress is introduced to the surface since the elongation is elastically restrained from the surrounding part. It is reported that peening is effective in improving the fatigue life [7] and preventing SCC [8] by modifying the stress state of the surface in such a process.

The strength and number of impacting load can influence the residual stress distribution after peening since the compressive stress is introduced by the impulsive load. So, the residual stress distribution after peening was predicted in various reports [9-11]. In these reports, mechanical behavior under the collision of a shot is investigated using elastic plastic analysis. Since the dimension of shot is 1mm or smaller and the duration of collision of shot is several micro seconds, very high resolution for space and time is necessary to predict the collision of shot. So, the prediction of the residual stress distribution for the entire of the target is very difficult in the point of analysis scale. Furthermore, in order to discuss the effect of peening on the modification of an analysis method is proposed to welding residual stress, it is necessary to consider the residual stress generated by the welding. This will make the simulation more difficult.

On the other hand, to conduct a large scale analysis of welding mechanical problem, the authors have proposed the Idealized Explicit FEM (IEFEM) [12-13]. IEFEM is developed based on dynamic explicit FEM and realizes fast and highly accurate analysis by considering the convergence to the static equilibrium state. In addition, since this method is based on the dynamic explicit FEM, It has a high applicability to parallelization. It has been reported that much faster analysis than conventional methods can be achieved by introducing parallelization using a graphics processing unit (GPU). So an efficient analysis can be expected by using IEFEM and we have proposed an analysis system to analyze the residual stress after shot peening using Idealized Explicit FEM [14].

Therefore, in this study, in order to construct an analysis method, we extend the Idealized Explicit FEM to consider the dynamic effect due to the impact load. Next, a load model of the impact load due to the collision of a shot is also proposed. The validity of the proposed analysis method is investigated by applying the proposed method to the shot peening of the Almen strip pieces [15]. Finally, the influence of the amount of shot collision on residual stress distribution is investigated by applying the proposed method to the modification of the residual stress distribution in the bead-on welded plate by shot peening.

ANALYSIS METHOD OF RESIDUAL STRESS DISTRIBUTION DURING SHOT PEENING

IDEALIZED EXPLICIT FEM CONSIDERING DYNAMIC EFFECT

In shot peening, 1 mm or smaller shots collide with the target surface numerous times and compressive stress is introduced. To predict the stress distribution under such a process, dynamic elastic plastic analyses with extremely high spatial resolution are necessary. Here, the proposed analysis system that can predict the residual stress distribution after shot peening by using the large-scale nonlinear mechanical analysis method named IEFEM [10], is briefly explained. The detailed formulations are found in the literature [12].

In dynamic elastic plastic analyses using IEFEM, the semi-discretized equation of motion by FEM is discretized for time by using Newmark's beta method and the linearized equation from the Newton-Raphson method. Equation (1) to (3) is defined as the fundamental equation:

$$\left[K_{eff}\right]{}^{(k)}\{\Delta U\} = {}^{(k)}\left\{F_{eff}\right\} \tag{1}$$

$$\left[K_{eff}\right] = \left(\frac{1}{\beta\Delta t^2}[M]+\frac{\gamma}{\beta\Delta t}[C]+[K]\right) \tag{2}$$

$$\left\{F_{eff}\right\} = \{F\}_{t+\Delta t} - [M]\ {}^{(k-1)}\left\{\ddot{U}\right\}_{t+\Delta t}[C]^{(k-1)}\left\{\dot{U}\right\}_{t+\Delta t} - {}^{(k-1)}\{Q\}_{t+\Delta t} \tag{3}$$

where, $[K_{eff}]$, $\{\Delta U\}$and $[F_{eff}]$ are the effective stiffness matrix, the displacement increment vector and the effective load vector, $[M]$ and $[C]$ are mass matrix and damping matrix, $\left\{\ddot{U}\right\}_{t+\Delta t}$, $\left\{\dot{U}\right\}_{t+\Delta t}$, $\{Q\}_{t+\Delta t}$ and $\{F\}_{t+\Delta t}$ are acceleration vector, velocity vector, internal force vector and load vector at time $t+\Delta t$, respectively. Upper left subscript (k) of each term means the iteration count.

To apply the procedures of Idealized Explicit method, the following equation is assumed by adding virtual inertial term and damping term at virtual time τ to Eq. (1).

$$[M_{dum}]\left\{\ddot{U}_{dum}\right\}_{\tau}+[C_{dum}]\left\{\dot{U}_{dum}\right\}_{\tau}+\left[K_{eff}\right]\{U_{dum}\}_{\tau}=\left\{F_{eff}\right\}_{\tau} \tag{4}$$

Discretizing Eq. (2) by the central difference and advancing the time steps until the virtual inertial term and the virtual damping term become negligibly small, that is, advancing the virtual time τ in Eq. (4), enables the displacement vector to be obtained. The displacement vector obtained by advancing the virtual time τ is used as a solution. By using these steps, it is expected that the same solution as that by solving Eq. (1) using the iteration method (Newton-Raphson method) can be obtained. The virtual mass matrix $[M_{dum}]$ and the virtual damping matrix $[C_{dum}]$ are utilized only to obtain the converged solution. The formulation of these matrices, which can reduce the number of time steps for convergence, are employed as shown in [8].

EQUIVALENT LOAD MODEL

A load on the collision of a shot is considered in the above dynamic elastic plastic analysis method based on IEFEM, and the analysis system of the mechanical behavior during shot peening is constructed. As shown in Fig. 1, the history of the load distribution during the collision of a shot is modeled as an equivalent load model [13], which is introduced as an external force. The equivalent load model is expressed as the product of the load distribution function defining the shape of the load distribution, and the load history function defining the amount of the colliding load as shown in the following equation:

$$P(\rho,\tau) = f(\rho,\tau) \cdot g(\tau) \tag{5}$$

where, ρ, τ , $P(\rho,\tau)$, $f(\rho,\tau)$ and $g(\tau)$ are defined as the normalized distance from the collision center, the normalized time from the beginning of collision, the load distribution history function, the load distribution function and load history function, respectively. ρ and τ are defined as follows:

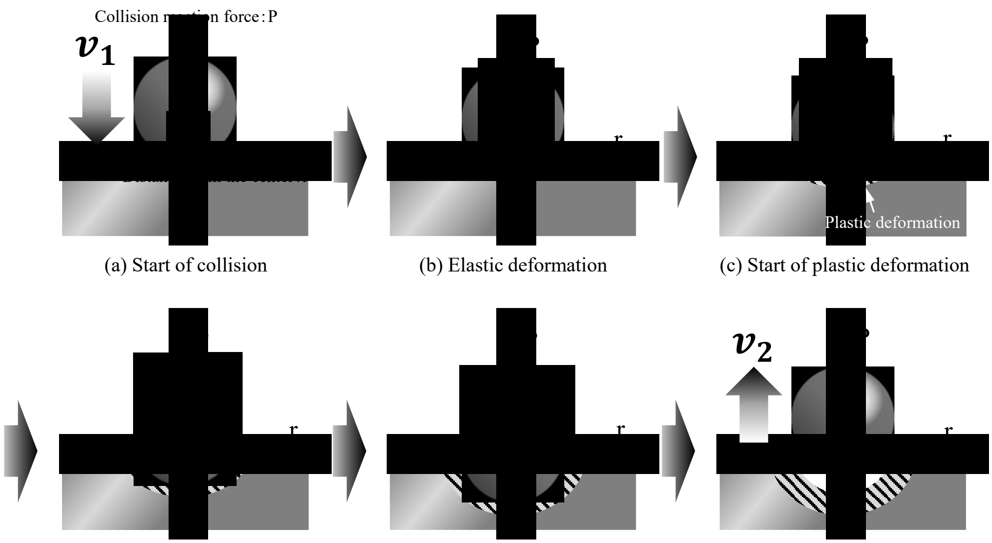

(a) Start of collision (b) Elastic deformation (c) Start of plastic deformation

(d) Plastic deformation (e) End of plastic deformation (f) End of collision

Fig. 1 Schematic illustration of reactive force for each stage of shot collision.

$$\rho = \frac{r}{r_0} \ , \tau = \frac{t}{t_0} \tag{6}$$

where r and r_0 are the distance from the collision center and the shot radius, and t and t_0 are the time from the beginning of the collision and the duration of the collision, respectively. The load distribution function and the load history function are defined as the functions that can reproduce the reaction force distribution obtained by the analysis of the collision of a single shot considering contact[14].

INDICATORS USED IN THE PROPOSED METHOD

The amount of the projected shot in shot peening is expressed by coverage in the Almen strip test. To simulate the Almen strip test, the corresponding index to the coverage in the numerical analysis is proposed. The definition formula of the coverage obtained by the experiment is shown in the following equation. The coverage means the area ratio of the shot collision area to the area of the shot collision surface. It is understood that it corresponds to the surface equivalent plastic strain ratio defined as follows;

$$Coverage = \frac{S}{A} \ (coverage < 100\%) \tag{7}$$

Where A is the area of the target surface of shot projection and S is the area of the shot impression. After the coverage reaches 100%, the following definition is used.

$$Coverage = 100(\%) \times \frac{t}{t_{100\%}} (coverage \geqq 100\%) \tag{8}$$

Where t is shot projection time, and $t_{100\%}$ is the time required for the coverage to reach 100(%). Regarding the coverage, the coverage is 200% at the time when the shot projection amount was doubled from the time required for the coverage of 100%, and the coverage is 300% when tripled.

Next, in order to clarify the relationship between the equivalent plastic strain on the target surface of the shot peening and the coverage in the proposed analysis system, the surface equivalent plastic strain rate *Cv* is defined as Eq. (9).

$$Cv = \frac{\bar{\varepsilon}^p_{surface}}{\bar{\varepsilon}^p_{single}} \tag{9}$$

$$\bar{\varepsilon}^p_{surface} = \frac{\int_{A_t} \bar{\varepsilon}^p dA}{\int_{A_t} dA} \tag{10}$$

$$\bar{\varepsilon}^p_{single} = \frac{\int_{A_s} \bar{\varepsilon}^p dS}{\int_{A_s} dA} \tag{11}$$

Here, $\bar{\varepsilon}^p_{surface}$is the average of the equivalent plastic strain on the target surface of shot penning, and $\bar{\varepsilon}^p_{single}$ represents the average of equivalent plastic strain on the surface due to a single shot. A_s and A_t represents the impression area of a single shot and the target surface, respecyively. The definition of *Cv* by Eqns. (9)-(11) is used for the *Cv* less than 1.0 (100%). For more than 1.0 of *Cv*, $Cv = t/t_{Cv=1.0}$ is used in the same way as the coverage. Here, $t_{Cv=1.0}$ is the time required for *Cv* to reach 1.0.

PERFORMANCE OF THE PROPOSED METHOD

ANALYSIS MODEL AND CONDITIONS

Figure 2 shows analysis model. The dimension of model is 76.0 mm in length, 19.0 mm in width, 1.3 mm in thickness, The model is meshed with 0.2 mm intervals in the longitudinal direction and the width direction and meshed with 0.1625mm intervals in the thickness direction. The material was assumed to be high speed steel (SKH51, JIS G4403:2006) for the specimen and SUS 304 for the shot. The material constants obtained by the tensile test is shown in Table 1. The diameter of the shot was set to 0.8mm, and the velocity of shot projection is set to be 30 mm/s. Fig. 3 shows the schematic diagram of the experimental procedure of the shot peening teset using the Almen strip piece. In the analysis, shots were projected until the surface equivalent plastic strain rate Cv reached 500%. In the test using Almen strip piece, shot peening is carried out under the constraint as shown in Fig. 3.

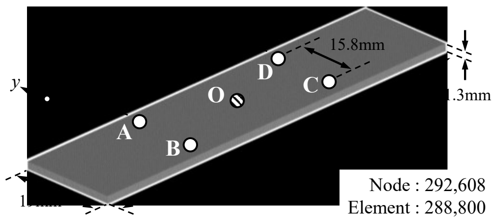

Fig. 2 Analysis model and measurement position of Arc height.

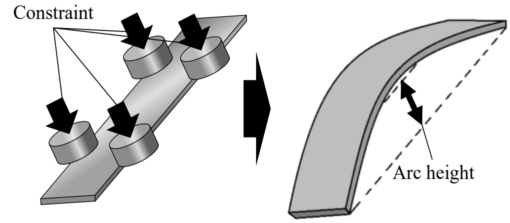

(a) During shot peening (b) After shot peening

Fig. 3 Schematic illustration of Experimental procedure of Almen strip.

Table 1 Material constant of High-speed-steel and SUS304.

	High-speed-steel	SUS304
Density (kg/m³)	7.92×10^3	7.90×10^3
Young module (MPa)	201086	198500
Poisson ratio	0.300	0.294
Initial yield stress (MPa)	1450.0	288.0
Work hardning (MPa)	15485.0	1474.0

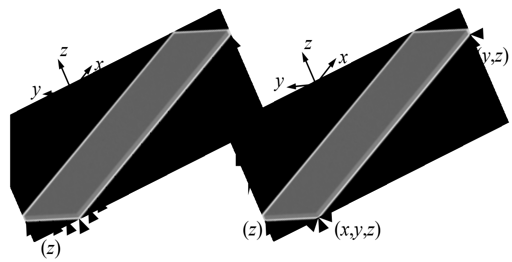

(a) During shot peening (b) After shot peening

Fig. 4 Schematic illustration of Analysis procedure of Almen strip.

After the shot peening, the constraint is released the arc height is measured. To simulate these procesures, the following procedure is adopted in the analysis. First, the analysis of shot peening is conducted under which the backside of the specimen is constrained in the out-of-plane direction during shot peening. And static analysis is conducted to determine the arc height. After that, the constraint is released. The arc height was calculated from the distance between the plane formed by points A, B, C and D and O point shown in Fig. 2.

ANALYSIS ACCURACY

Fig. 5 shows the displacement distribution in the out-of-plane direction at the surface equivalent plastic strain rate *Cv* = 100, 300, and 500 (%). From the figure, it can be confirmed that the displacement in the out-of-plane direction increases with the increase of the surface equivalent plastic strain rate *Cv*. Since the elogating plastic strain in the in- plane direction on the target surface due to the peening will cause the difference of the elogation between the back and front surface, a bending deformation in out-of-plane direction can occur.This can lead to the occurrence of the arc height.

Fig. 6 shows the relation between the arc height and the surface wquivalent plastic strain rate Cv defined in analysis. The figure indicates that the increase of the arc height is large in the small Cv and that in the large Cv is small. the plastic deformation amount is small, the influence of work hardening is small because the influence of work hardening increases as the amount of plastic strain increases, Since the yield stress is also small, plastic deformation is likely to occur, but as the surface equivalent plastic strain rate Cv increases, the plastic deformation of the surface increases, so the effect of work hardening increases and the yield stress increases, so the amount of occurrence of plastic deformation Becomes small, which is considered to be small. So, plastic deformation tends to occur because the

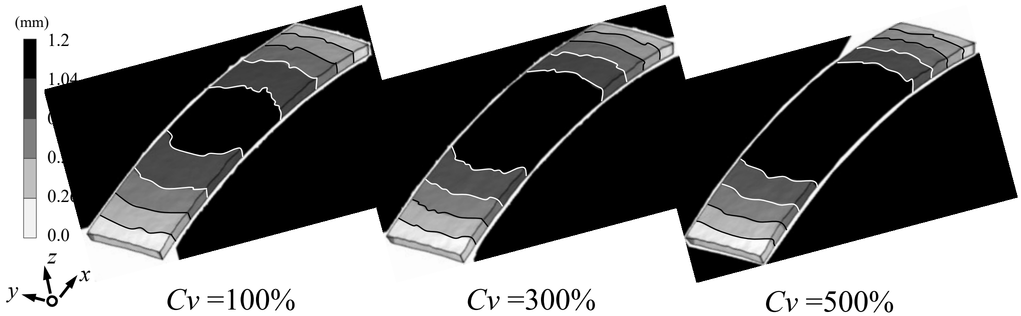

Fig. 5 Distribution of out-of plane deformation in each *Cv*.

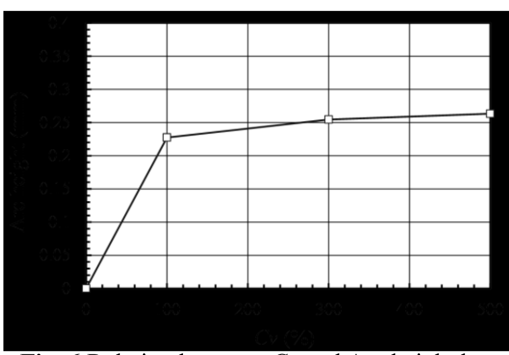

Fig. 6 Relation between *Cv* and Arc height by analysis.

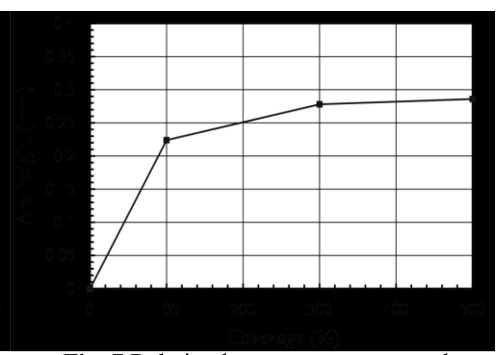

Fig. 7 Relation between *coverage* and Arc height by experiment.

yield stress is also small. However, as the surface equivalent plastic strain rate *Cv* increases, the plastic deformation of the surface increases, so the effect of work hardening increases and the yield stress increases. Therefore, it is considered that the amount of occurrence of plastic deformation becomes small.

Fig. 7 shows the relation between the coverage and the arc height of the Almen strip piece obtained by the measurement. Comparing Figs. 6 and 7, it can be seen that the tendency of the arc height up to *Cv* and coverage are in good agreement; the increase of the arc height is large in small *Cv* and coverage, and that in large *Cv* and coverage is small. In addition, the amount of the arc height is in good agreement. As shown in the above discussion, it is found that the relation between the proposed indicator Cv and the arc height can well reproduce that between the coverage and the arc height.

APPLICATION TO BEAD-ON-PLATE JOINT

ANALYSIS MODEL

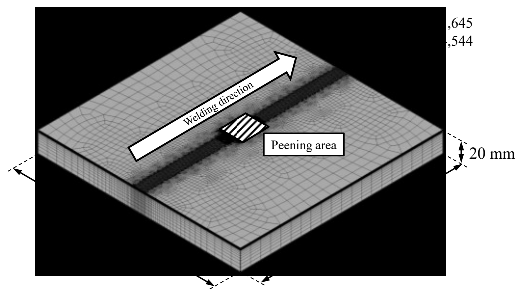

(a) Overall of analysis model.

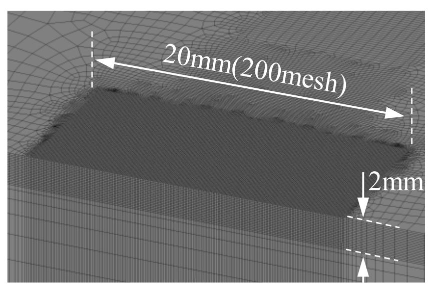

(b) Zoomed view of peening area

Fig. 8 Analysis model.

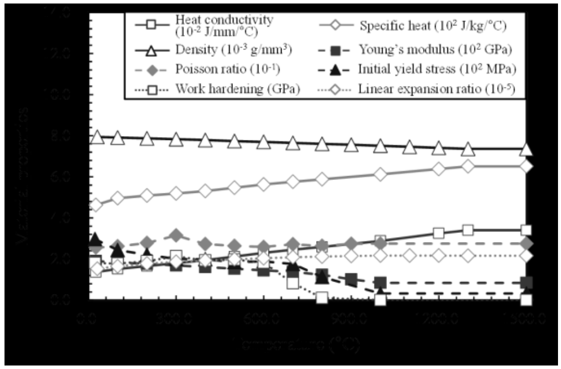

Fig. 9 Material properties of SUS316L.

In this chapter, the relaxation behavior of welding residual stress by shot peening is predicted. The proposed method is applied to the residual stress distribution of the bead-on-plate weld specimen. The analysis model is shown in Fig. 8 (a). The demension of themodel is 200mm in length, 200mm in width, 20mm in thickness. The number of nodes is 2,451,645, the number of elements is 2,374,544, and the number of degrees of freedom is 7,280,810. The material is assumed as SUS316L. The welding condition assumed in this analysis is as follows; the current is 180A, the voltage is 10V, speed is 3.33mm/s and the heat efficiency is 0.7. As shown in Fig. 8 (b), the 20 mm × 20 mm portion of the center of the model was defined as the collision area of the shot. The collision area was meshed with the interval of 0.1 mm in the welding line direction and the width direction. The assumed temerature dependence of material propaties of SUS316L is shown in Fig. 9. The procedures of this analysis is as follows; first, welding residual stress is predicted using thermal elastic plastic analysis method based on IEFEM. And, the shot peening process is analyzed by the proposed analysis system and the modification of stress distribution due to shot peening is investigated. As the condition of peening, the material of the shot is assumed as SUS 304, and analysis is performed until the surface equivalent plastic strain rate Cv defined in the previous section reaches 150%.

ANALYSIS RESULTS

Figure 10 shows the residual stress distribution on the wid cross section along the welding line at the end of welding. Fig. 10 (a) shows the residual stress distribution in the direction

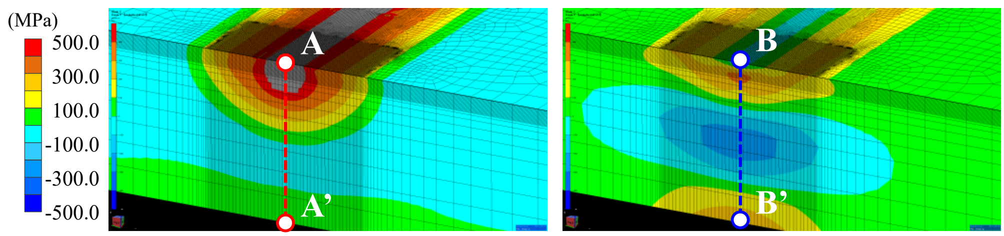

(a) σ_{xx}. **(b)** σ_{yy}.

Fig. 10 Distribution of stress in *x* direction and *y* direction before peening.

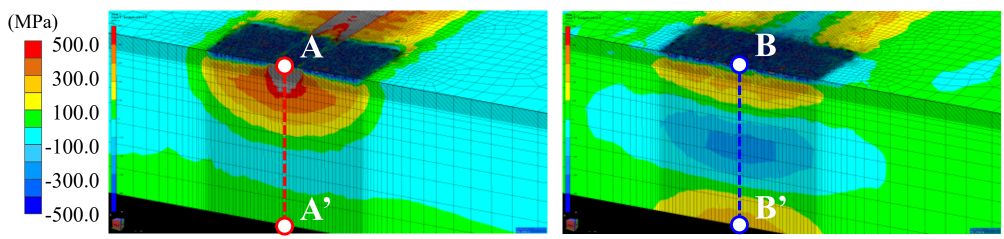

(a) σ_{xx}. **(b)** σ_{yy}.

Fig. 11 Distribution of stress in *x* direction and *y* direction for after peening.

of the weld line, and Fig. 10 (b) shows the residual stress distribution in the direction perpendicular to the weld line. From Fig. 10 (a) and (b), it can be seen that strong tensile residual stress occurs particularly near the surface due to the welding. Fig. 11 shows the stress disribution after the shot peening on the same cross section as Fig. 10. Fig. 11 (a) shows the residual stress distribution in the weld line direction, and Fig. 11 (b) shows the residual stress distribution in the direction perpendicular to the weld line. From Figs. 10 and 11, it is found that the tensile residual stresses in both the welding line direction and the vertical direction to the welding line, changed to strong compressive residual stress especially on the target surface by the shot peening.

Fig. 12 shows the distribution of stress in weld line direction along line A-A´. In Fig. 12, diamonds with solid line indicates the as-weld stress. Squares with dotted line and squares with solid line show the stress in weld line direction at *Cv*=75%, 150%, respectively. In addition, triangles with dotted line shows these at *Cv*=150% which considers no welding residual stress. From the figure, it is found that the difference between the stress distribution at as-weld and that at *Cv*=75% is large and with the increase of coverage, the compressive

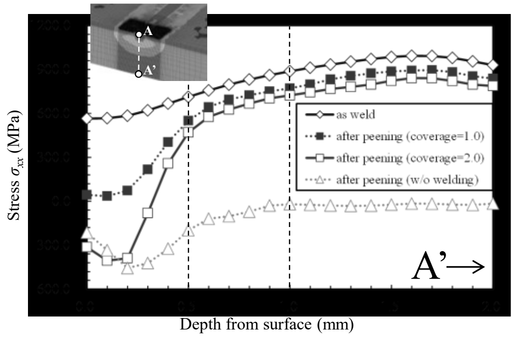

Fig. 12 Distribution of residual stress in *x* direction for each coverage.

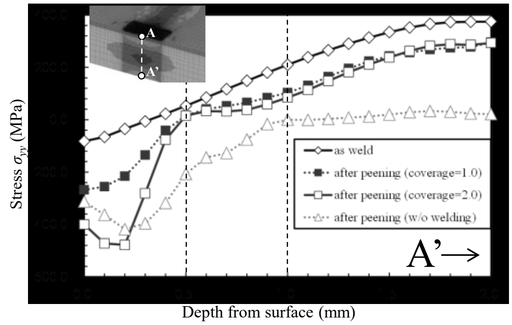

Fig. 13 Distribution of residual stress in *y* direction for each coverage.

stress in peening region becomes larger. From the comparison of stress distribution between with and without welding residual stress at *Cv*=150%, it is shown that the both stress distributions is similar in the peened region. Fig. 13 shows the distribution of stress in the vertical direction to the welding line along line A-A′ in the same way as Fig. 12. From the figure, the same tendency as stress in welding direction is found: the compressive stress in the peening region becomes larger with the increase of coverage.

CONCLUSIONS

In this research, to predict the effect of the modification of residual stress distribution due to shot peening, the authors proposed an amalysis system and an indicator to quantitatively evaluation the effect of shot peening. In order to verify the validity of the proposed method, the arc height in the test using the Almen strip piece was compared by experiment and analysis. The proposed analysis system was also applied to the prediction of the modification of residual stress distribution in bead on plate model. As a result, the following results were obtained:

- From the analysis and experiment of the test using Almen strip pieces, it was confirmed that the arc height increase largely under small coverage, while the increase of arc height becomes small in large coverage both in the analysis and experiment. And it was also found that the proposed indicator Cv which corresponds to the coverage can well reproduce the relation between the coverage and the arc height.
- Shot peening to the Almen strip piece was analysed by the proposed method. As a result, it was confirmed that the arc height obtained by the experiment agrees well with those by the analysis. In addition, it was confirmed that the coverage in the experiment corresponding to each arc height and the *Cv* in the analysis also agree well. By using the surface equivalent plastic strain rate *Cv*, we confirmed that it can be arranged like the coverage obtained by the experiment.
- To analyse change due to shot peening of weld residual stress distribution, Idealized Explicit method FEM was applied to the analysis of residual stress at

bead on plate and applied development method to the obtained residual stress distribution. As a result, it was confirmed that there was a difference in stress change between *Cv*=75% and 150%. The number of elements, the number of nodes and degrees of freedom of the model used for the above analysis were 2,374,544, 2,451,645, and 7,280,810 respectively.

REFERENCES

[1] A. OHTA, N. SUZUKI, Y. MAEDA: Unique fatigue threshold and growth properties of welded joints in a tensile residual stress field, *International Journal of Fatigue*, Vol.19, No.93 (1997), pp.303-310.

[2] P. A. DESCHÊNES, J. LANTEIGNE, Y. VERREMAN, D. PAQUET, J. B. LÉVESQUE, M. BROCHU: A new experimental method to study the influence of welding residual stresses on fatigue crack propagation, *International Journal of Fatigue*, Vol.100, No.1 (2017), pp.444-452.

[3] Z. LU, L. SHI, S. ZHU, Z. TANG, Y. JIANG: Effect of high energy shot peening pressure on the stress corrosion cracking of the weld joint of 304 austenitic stainless steel, *Materials Science and Engineering,* Vol.637, No.18 (2015), pp.170-174.

[4] S. BAGHERIFARD, R. GHELICHI, M. GUAGLIANO: On the shot peening surface coverage and its assessment by means of finite element simulation: a critical review and some original developments, *Applied Surface Science*, Vol.259 (2012), pp.186-194.

[5] Y. SANO, N. MUKAI, K. OKAZAKI, M. OBATA: Residual stress improvement in metal surface by underwater laser irradiation, *Nuclear Instruments and Methods in Physics Research Section B*, Vol.121 (1997), pp.432-436.

[6] H. SOYAMA, O. TAKAKUWA: Enhancing the aggressive strength of a cavitating jet and its practical application, *Journal of Fluid Science and Technology*, Vol.6, No.4 (2011), pp.510-521.

[7] J. SAKAMOTO, Y. LEE, S. CHEONG: Effect of surface flaw on fatigue strength of shot-peened medium-carbon steel, *Journal of Engineering Fracture Mechanics*, Vol. 133(2015), pp.99-111.

[8] A. TELANG, A.S.GILL, S. TEYSSEYRE, S. R. MANNAVA, D. QIAN, V. K. VASUDEVAN: Effects of laser shock peening on SCC behavior of Alloy 600 in tetrathionate solution, *Journal of Collision Science*, Vol. 90(2015), pp.434-444 .

[9] M. KLEMENZ, V. SCHULZE, I. ROHR, D. LOHE: Application of the FEM for the prediction of the surface layer characteristics after shot peening, *Journal of Materials Processing Technology*, Vol.209 (2009), pp.4093-4102.

[10] M. KLEMENZ, V. SCHULZE, I. ROHR, D. LOHE: Application of the FEM for the prediction of the surface layer characteristics after shot peening, *Journal of Materials Processing Technology*, Vol.209 (2009), pp.4093-4102.

[11] B. BHUVARAGHAN, S. M. SRINIVASAN, B. MAFFEO, R. D. MCCLAIN, Y. POTDAR, O. PRAKASH: Shot peening simulation using discrete and finite element method, *Advances in Engineering Software*, Vol.41 (2010), pp.1266-1276.

[12] K. IKUSHIMA AND M. SHIBAHARA: Prediction of residual stresses in multi-pass welded joint using Idealized Explicit FEM accelerated by a GPU, *Computational Materials Science,* Vol.93 (2014), pp.62-67.

[13] M. SHIBAHARA, H. SERIZAWA AND H. MURAKAWA: Finite element method for hot cracking using interface element (3rd report) - development of static-dynamic hybrid method, *Journal of Kansai Society of naval Architects Japan*, No.235 (2001), pp.161-169.

[14] K. IKUSHIMA, M. SHIBAHARA, K. AKITA, H. SUZUKI, S. MOROOKA, S. NISHIKAWA, T. FURUKAWA: Numerical analysis of residual stress distribution on peening process, *Welding in the World*, VOL.61, No.3 (2017), pp.517-527.

[15] O. UNAL: Optimization of shot peening parameters by response surface methodology, *Journal of Surface & Coatings Technology*, Vol. 305(2016), pp.99-109